NUCLEAR INSTRUMENTS AND METHODS 127 (1975) 173–182; © NORTH-HOLLAND PUBLISHING CO.

A PRECISION LUMINOSITY MONITOR FOR USE AT ELECTRON–POSITRON STORAGE RINGS*

J. F. CRAWFORD+, E. B. HUGHES, L. H. O'NEILL and R. E. RAND†

High Energy Physics Laboratory and Department of Physics, Stanford University, Stanford, California 94305, U.S.A.

Received 8 April 1974

A precision luminosity monitor is described which has been used successfully in an experimental test of quantum electrodynamics at the 2.6 GeV electron–positron storage ring (SPEAR-I) at the Stanford Linear Accelerator Center. Design considerations and construction details are given, together with a discussion of radiative corrections and an evaluation of the response of the monitor.

1. Introduction

Tests of quantum electrodynamics (QED) at high-energy electron–positron storage rings are frequently based upon comparisons of the measured rates of reactions such as $e^+e^- \to e^+e^-$ (Bhabha scattering), $e^+e^- \to \gamma\gamma$, or $e^+e^- \to \mu^+\mu^-$ at large scattering angles, usually in the range 40° to 140°, with the rate of either Bhabha scattering at small angles (of the order of 3°) or the rates of either single or double bremsstrahlung. Unlike the rates at large angles, which involve the maximum-possible four-momentum transfer, the rates at the small angles are dominated by relatively small values of momentum transfer for which the validity of QED is already well established. The instrumentation used to detect the small-angle process, whatever it may be, is commonly called a luminosity monitor, and it is the purpose of this article to describe the design of the precision luminosity monitor used in a recent test of QED at the 2.6 GeV electron–positron storage ring (SPEAR-I) at the Stanford Linear Accelerator Center and to give an assessment of its performance. This monitor is based upon the detection of Bhabha scattering near 3.7° and the design goal was to provide a device whose response was accurate to within a systematic uncertainty of about ±2%.

The detailed design considerations for the monitor are described in section 2 of this paper, and a description of the monitor construction is given in section 3. A summary of the operating procedure is contained in section 4, and radiative corrections are discussed in section 5. An evaluation of the response of the monitor at SPEAR-I is given in section 6 and finally, in section 7, the application of the monitor to higher-energy storage rings such as SPEAR-II (the improved version of SPEAR-I with a maximum operating energy of 4.2 GeV) and modifications to incorporate diagnostic features suggested by the operating experience at SPEAR-I are discussed.

2. Design considerations

Bhabha scattering, as opposed to single or double bremsstrahlung, was chosen as the reference reaction, because the detection efficiency and useful aperture are more readily defined for electrons than for γ-rays, because the location of the necessary instrumentation is more compatible with the design of SPEAR-I, and because both the single- and double-bremsstrahlung reactions are expected to suffer from substantial backgrounds[1]) (the former from gas bremsstrahlung and the latter, especially at high luminosities, from accidental coincidences due to single bremsstrahlung). The principal design considerations were that the response of the monitor be as insensitive as possible both to manufacturing tolerances and to the parameters of the storage ring. In the latter category it is immediately clear that the luminosity measurement must be insensitive to the longitudinal intensity profile of the luminous region. At SPEAR-I the luminous region is produced by the overlap of single bunches of electrons and positrons, each of which has a Gaussian longitudinal profile with a width dependent on the circulating current. Typically, immediately after injection, the circulating current in each beam is about 40 mA and this is allowed to decay to about 15 mA before the next injection cycle begins. During this interval the full width at half maximum (fwhm) of each bunch decreases from 22″ to 17″, and the fwhm of the luminous

* Work supported in part by the National Science Foundation Grant GP-38611.

+ Presently at CERN, 1211 Geneve 23, Switzerland.

† Presently at University of Western Australia, Nedlands, Western Australia 6009.

region, which is approximately Gaussian[2]), decreases from 16″ to 12″. The design of the monitor must be such that changes in the source size of this magnitude are not strongly reflected in its response.

The rate R at which Bhabha events are detected by a counter looking at the luminous region is given by the relation $R = L\sigma$, where σ is the cross section for Bhabha scattering integrated over the aperture of the counter, and L is the luminosity of the storage ring. If charge measurements are not made on the detected particles, then the differential cross section for Bhabha scattering at an angle θ can be written as follows:

$$\frac{d\sigma_B}{d\Omega} = \frac{\alpha^2}{8E^2} \frac{(2-\sin^2\theta)\,(4-\sin^2\theta)^2}{\sin^4\theta}, \qquad (1)$$

or, to second order in θ:

$$\frac{d\sigma_B}{d\Omega} = \frac{4\alpha^2}{E^2\theta^4}(1-\tfrac{1}{3}\theta^2). \qquad (2)$$

If counters small enough to be conveniently installed are used to detect the scattered particles, the scattering angle must be restricted to not more than about 5° in order to provide an adequate counting rate. It then becomes necessary to know the scattering angle θ with very high precision. If, as in the present design, counters located at a nominal transverse distance of 5″ from the beams are used to detect Bhabha events at an angle $\theta = 3.7°$, then an uncertainty of 1% is incurred in the observed luminosity due to an uncertainty of only 0.012″ in the transverse position of the luminous region. This is a fundamental problem, since the beams themselves can easily move by this amount during normal operation of SPEAR-I.

Our solution is based on a suggestion of Barbiellini et al.[3]), and is shown schematically in fig. 1, and more realistically in fig. 2. Consider first the two identical small counters P_1 and P_4. The rate of Bhabha events detected by P_1, neglecting the second-order term in eq. (2), is $R_1 = Lk/\theta^4$, where k is a constant determined by the beam energy and the solid angle subtended by P_1 at the interaction region. Similarly, the rate in P_4 is $R_4 = kL/\theta^4$. If the luminous region is displaced radially by an amount δx, then P_1 and P_4 will detect Bhabha events at angles of $(\theta+\delta\theta)$ and $(\theta-\delta\theta)$, respectively, where $\delta\theta \simeq \delta x/D$. The rates in P_1 and P_4 will then be

$$R_1 = kL/(\theta+\delta\theta)^4,$$

and:

$$R_4 = kL/(\theta-\delta\theta)^4.$$

The average rate in P_1 and P_4, to second order in $\delta\theta$, will then be:

$$\bar{R} = \tfrac{1}{2}(R_1+R_4) = \frac{Lk}{\theta^4}\left\{1+10\left(\frac{\delta\theta}{\theta}\right)^2\right\} \qquad (3)$$

$$= \frac{kL}{\theta^4}\left\{1+10\left(\frac{\delta x}{d}\right)^2\right\}. \qquad (4)$$

If the two counters P_1 and P_4 are rigidly located relative to each other on a common mounting bar, it follows from eq. (4) that the average rate in P_1 and P_4 depends only in second order on radial displacements of the luminous region. If, as in fig. 1, $d = 5''$ and $D = 80''$, it is necessary that the luminous region be displaced by 0.05″ in x in order to change the average rate by 0.1%. Moreover, such a displacement in x would cause the rates in P_1 and P_4 to differ by 8%, which should be readily observable. Identical considerations apply also to the counter pair P_2 and P_3. Similarly, it can be easily shown that if the luminous region is rotated about the y axis, the average rate in P_1 and P_4 (and in P_2 and P_3) depends only in second order on such rotations. Specifically, a rotation of 0.6 mrad is required in order to change the average rate by 0.1%. Such a rotation would also cause the rates in P_1 and P_4 to differ by 8%, but, in contrast to a displacement of the luminous region in x, the relative rates in P_2 and P_3 would change by an equal but opposite amount to those in P_1 and P_4.

If, on the other hand, the luminous region is displaced vertically by an amount δy, then P_1 and P_4 will each detect Bhabha events at an angle:

$$\theta' = \left\{\theta^2+\left(\frac{\delta y}{D}\right)^2\right\}^{\frac{1}{2}} \simeq \theta\left\{1+\tfrac{1}{2}\left(\frac{\delta y}{d}\right)^2\right\}, \qquad (5)$$

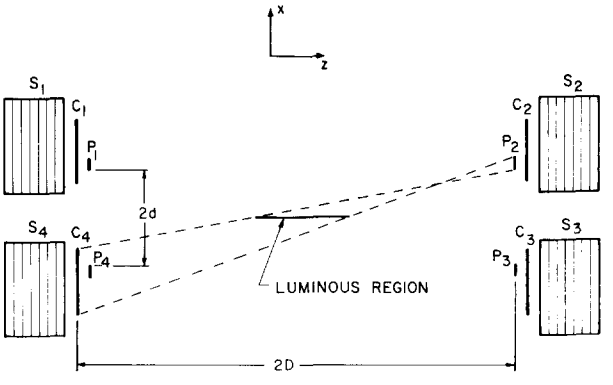

Fig. 1. A schematic diagram illustrating the operating principle of the monitor.

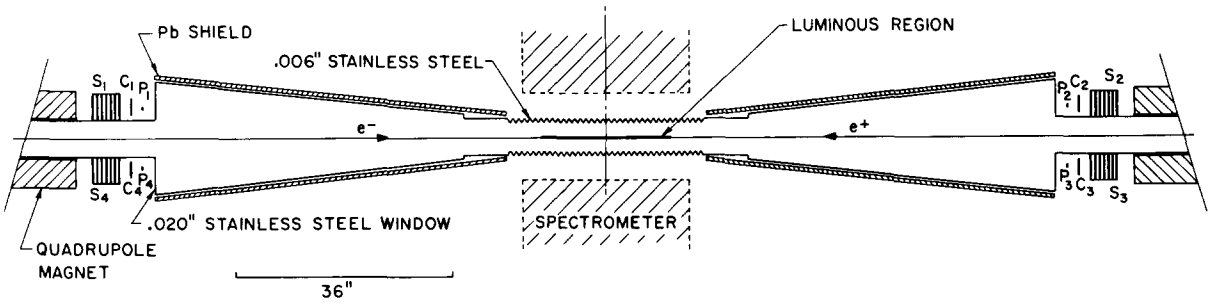

Fig. 2. A plan view of the luminosity monitor, showing the vacuum box and the locations of the monitor counters.

and the rate in each of these counters will be:

$$R = \frac{Lk}{\theta^4}\left\{1-2\left(\frac{\delta y}{d}\right)^2\right\}. \qquad (6)$$

It follows from eq. (6) that the detected rates in P_1 and P_4, and also in their average, depend only in second order on vertical displacements of the luminous region. A displacement in y of 0.11″ is required in order to change the rates by 0.1%. Identical considerations apply also to the counter pair P_2 and P_3. The detected event rates in P_1 and P_4 (and in P_2 and P_3) are also insensitive to rotations of the luminous region about the x axis. In this case, a rotation of 1.4 mrad is required in order to change the detected event rates by 0.1%.

By similar considerations it can be shown that the average rate detected by the counter pair, P_1 and P_2, depends only in second order on displacements of the luminous region in the longitudinal direction. For the specified values of the distances d and D, it is necessary that the luminous region be displaced by 2.5″ in z in order to change the average detected rate by 0.1%. Moreover, such a displacement would cause the rates in P_1 and P_2 to differ by 14%, which again should be readily observable. Identical considerations apply also to the counter pair P_3 and P_4. It can also be easily shown that the rate in any P counter is only affected in second order by changes in the length of the luminous region. For example, these rates would change by only 0.5% as the fwhm of the luminous region is decreased from 16″ to 12″.

It is evident from the above considerations that the sum of the event rates in the four P counters provides a luminosity measurement that is insensitive to displacements and rotations of the luminous region and also to changes in its longitudinal profile. Moreover, the relative changes that occur in the four individual P-counter rates reflect the degree to which displacements in x and z or rotations about the y axis occur. At SPEAR-I it is known from measurements made with beam-position monitors located $\pm 88''$ in z from the center of the luminous region, that the position of the luminous region can fluctuate by up to $\pm 0.02''$ in x and $\pm 0.004''$ in y, and that rotations of the luminous region of up to 0.35 mrad can occur about both the x and y axes. It is also expected that displacements δz of the luminous region in z should be much less than the widths in z of the circulating bunches, i.e., $\delta z \ll 8''$. From the foregoing analysis it is clear that the expected changes in the measured luminosity in response to all of these displacements and rotations is on the order of or less than 0.1%. Moreover, these small effects are calculable and are, therefore, quite unimportant. In principle, therefore, the precise measurement of luminosity is reduced to the geometric problem of defining the acceptance apertures of the four P counters and of determining the transverse and longitudinal separations between them. These factors will be discussed in section 3.

In order to identify Bhabha events at SPEAR-I in the presence of background radiations it was necessary to operate the P counters in coincidence with the complementary counters C and shower counters S shown in fig. 1. The purpose of each C counter was to detect the recoil particle from a Bhabha event detected by the opposite P counter, while the S counters placed a threshold requirement on the energies of both detected particles. Due to the length of the luminous region, the cross-sectional areas of the C and S counters have to be considerably larger than that of the P counters in order to detect Bhabha events with good efficiency. The C counters are large enough so that if a Bhabha particle hits a P counter, a collinear recoil particle would hit the appropriate C counter with greater than 99% probability. The small correction factor is a geometric effect due to the longitudinal profile of the luminous region, which in turn depends on circulating current. However, both the profile of the luminous region and its variation with current are sufficiently well known that

the associated uncertainty in the luminosity is reduced to much less than 0.1%.

3. Monitor construction

The monitor counters were operated in conjunction with a specially designed vacuum box, which is shown in fig. 2. The center section of this box consists of corrugated stainless-steel tubing of sufficiently small wall thickness (0.006″) that electrons and γ-rays can escape from the interaction region at large angles with only very small probabilities of generating secondary particles. The width of the vacuum box increases with distance from the luminous region so that Bhabha particles scattered at small angles can be detected in the monitor counters after passing through only thin (0.02″ stainless-steel) exit windows in the box. The sizes of both the monitor counters and the vacuum box were determined in detail by the requirements that they be compatible with the parameters of both the storage ring and the large-angle spectrometers. The corrugated steel tubing was available in standard lengths of 17.5″, and a minimum of two sections had to be used to cover the full aperture of the spectrometers. This condition set an upper limit of 103 mrad on the angular acceptance of the monitor. A lower limit of 42 mrad was set by the cross section of the SPEAR vacuum pipe at the quadrupole magnets closest to the interaction region, which in turn is determined by the cross section required during injection into the storage ring. The choice of locating the monitor counters in the horizontal plane rather than the vertical was made to leave the vertical plane free for the large-angle spectrometers, on the assumption that the background radiations from SPEAR would be more intense in the horizontal plane. The size of the vacuum box was limited in the vertical direction to allow maximum freedom of movement in the vertical plane for the large-angle spectrometers.

The dimensions and nominal positions of all the monitor counters are summarized in table 1. The height and width of the C counters were set by the size of the exit windows in the vacuum box. The P-counter dimensions were then determined by the requirement that the loss of events, assumed collinear, due to the recoil particle missing the C counter, be less than 1%. Due to the longitudinal profile of the luminous region the distribution of events in the plane of a C counter, corresponding to a point in the opposite P counter, is a line with an approximately Gaussian density profile of fwhm equal to 2.1″. This line is tilted from the horizontal for points in the opposite P counter above and below the plane of circulating beams. The C-counter dimensions then restrict the P-counter dimensions to those shown in table 1. As a consequence of this choice of counter dimensions the size and position of the C counter are much less critical to the luminosity measurement than are those of the P counter.

A thickness of 0.125″ was chosen for the P counters, and the vertical edges of these counters were shaped to equalize, as much as possible, the path lengths of all particles detected by these counters. In addition, the P counters were operated with a threshold pulse height approximately equal to one-half the minimum pulse height produced by fast charged particles at normal incidence. Under these conditions the uncertainty in the luminosity due to the P-counter thickness is less than 0.3%. In principle, this uncertainty can be reduced by the use of thinner P counters. However, with a thickness of 0.125″ only 15–30 photoelectrons are expected at the photocathode of the phototube coupled to each P counter. If this number were reduced, then difficulties could be experienced in operating the counters with good efficiency and in deriving fast-timing information. The geometrical effects of counter thickness are much less significant for the C counters and they were made with a thickness of 0.25″.

TABLE 1

A summary of the dimensions and nominal positions of all the monitor counters, including the test counter C_4'.

Counter	Dimensions (inches)			Longitudinal distance from center of luminous region (inches)	Transverse distance from central orbit to inside edge of counter (inches)
	height	width	thickness		
P	2.00	0.50	0.125	80	5.0
C	3.00	4.25	0.25	82	3.5
C_4'	2.63	3.00	0.25	82.25	4.1
S	4.00	5.25	4.75	82.5	3.1

The S counters consisted of lead–plastic scintillator sandwiches of total thickness equal to 10 radiation lengths. Each cell in these counters consisted of a lead plate 0.25″ in thickness and a plastic scintillator plate 0.25″ in thickness, and there were 9 cells in each counter. The height and width of the S counters were chosen such that the S counters extended beyond the edges of the associated C counters by two radiation lengths of lead, in order to provide good radial containment of the deposited energy for all Bhabha particles incident on the C counters. The energy resolution provided by these counters was approximately 30% fwhm.

The P-counter dimensions were determined to within 0.001″, which leads to an uncertainty of ±0.2% in the P-counter area and therefore, because there are four such counters, to an uncertainty of ±0.1% in the luminosity. The transverse separation between the P-counter pairs was known to within 0.005″, and the associated uncertainty in luminosity is ±0.14%. The longitudinal separation between the P-counter pairs was known to better than ±0.03″ out of 160″, and contributes a luminosity error of only ±0.03%. The C and S counters were located immediately behind the P counters. Since the positions of these latter counters were much less critical than those of the P counters, they were located to within 0.05″.

The vacuum chamber was fitted with 5.5″ diam. stainless-steel windows, 0.020″ in thickness, at each counter telescope. Since the window thickness is only 0.032 radiation lengths, the effect on the luminosity measurement was expected to be small. This was tested by inserting extra material, in the form of thin lead sheets, at the windows adjacent to the counters P_2 and P_3 and observing the change in the counting rates in these two channels of the monitor relative to the rates in the channels using counters P_1 and P_4. The results are shown in fig. 3 as a function of total window thickness. A least-squares analysis strongly favors a quadratic fit over a linear one. On this basis, the 0.020″ steel window is calculated to give 0.05% effect on the overall monitor rate, which is negligible.

Changes in the areas of the P counters and in their transverse separations due to thermal effects cause approximately equal but opposite changes in the measured luminosity. As a result, a temperature change of 30 °C causes a change of only 0.1% in the measured luminosity.

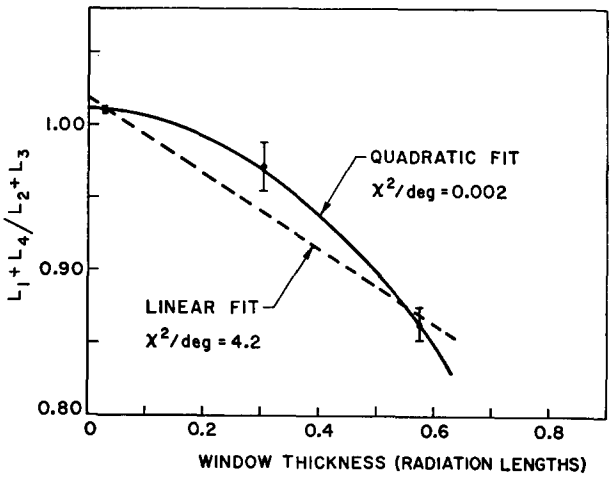

Fig. 3. A plot showing the ratio of the counting rates in two channels of the monitor as a function of the thickness of the windows of the vacuum box adjacent to counters P_2 and P_3. The rate L_1 indicates coincidences of the type $(P_1 \cdot S_1) \cdot (C_3 \cdot S_3)$, and similarly for L_2–L_4.

4. Operating procedure

Bhabha events were recognized by a coincidence between a P.S pair and the opposite C.S pair with an energy-threshold requirement of about 0.5 GeV in each S counter. Fig. 4 shows typical distributions of the relative timing of the P and C signals, with and without the S counters in coincidence. When the S counters are

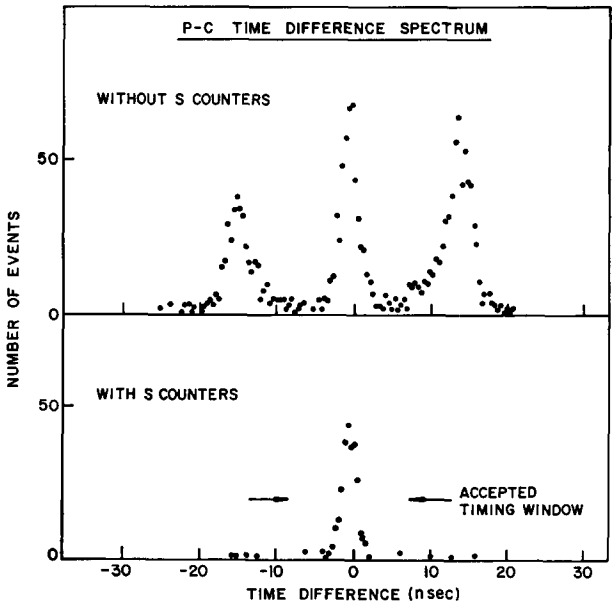

Fig. 4. Typical relative timing distributions observed between the P and C arms of a luminosity monitor channel. Top: without the use of the S counters; bottom: with the use of the S counters. The accepted timing window is indicated in the lower picture. The two distributions are not normalized to the same integrated luminosity.

not used in coincidence, the central peak is due in part (~50%) to Bhabha events and in part to background radiations associated with each of the travelling bunches, which can produce signals in (P.S) and (C.S) with the same relative timing as do the Bhabha events. The satellite peaks are caused by the background radiations associated with one of the two bunches, producing signals first in one counter and then in the other. Only coincidences with the relative timing expected for Bhabha events were accepted in practice. When the S counters are used in coincidence, the satellite peaks disappear and the central peak is dominantly due to Bhabha events. In practice, it was found that an average of 10% of the (P.S)·(C.S) rates with the correct relative timing were not due to Bhabha events but to the background radiations. Accordingly, the (P.S) signals were delayed by the orbit period and put into coincidence with the corresponding (C.S) signal. This gave a measure of the background rate, which was then subtracted.

The experiment was run at an energy of 2.6 GeV per beam for an integrated luminosity of 2.7×10^{36} cm^{-2}. The typical initial luminosity immediately after injection and collision of the beams was 5×10^{30} cm^{-2} s^{-1}, and the luminosity lifetime was about 1.8 h. The background rate in the monitor changed considerably during a typical injection cycle. Immediately after injection and collision of the beams the background rate was frequently as large as the true Bhabha rate. Usually, the background rate fell rapidly in the first few minutes to a level of approximately 20% of the true signal, and thereafter fell slowly to about 5% at the end of the cycle. Fig. 5 shows the luminosity versus time over a period of about 6 h towards the end of the experiment when the highest initial luminosities were recorded. Information such as that shown in fig. 5 was available on-line during the experiment and could be used, for example, to determine the optimum time at which to refill the storage ring.

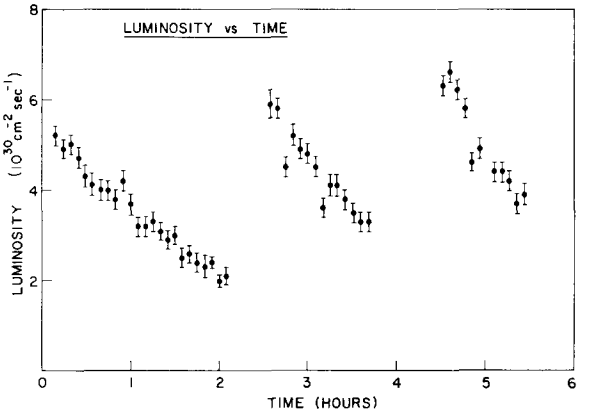

Fig. 5. A plot showing the observed luminosity over a typical period of 6 h. Each point represents the average luminosity over a 5 min interval.

During each injection cycle at SPEAR a total of approximately 1500 Bhabha events was detected by the sum of the four monitor channels, but the number of Bhabha events detected at large angles was never more than 100, and the numbers of $e^+e^- \to \gamma\gamma$ and $e^+e^- \to \mu^+\mu^-$ events were even smaller. The statistical error on the integrated luminosity measurements for each major partition of the experiment at large angles was never larger than 0.5% and therefore much smaller than the statistical error on the event numbers observed at large angles.

5. Radiative corrections

The differential cross section for Bhabha scattering shown in eq. (1) is correct only to lowest order in the fine structure constant α. The rate of Bhabha events detected by the monitor, however, is influenced by higher-order contributions to the scattering process and these must be considered in the evaluation of the response of the monitor. The higher-order contributions include elastic and inelastic processes and both must be computed to the same order in α, in order to avoid divergences in the calculation of the modification, or radiative correction, to the rate expected in the lowest order (α^2). The overall effect on the response of the monitor can be computed from the work of Berends et al.[4]), who have provided the differential cross section for Bhabha scattering correct to α^3. This amounts to the approximation that at most one photon is radiated during the scattering process.

The modified cross sections of interest are defined by the trigger requirements for a Bhabha event to be detected by the monitor. Let:

$$\left(\frac{\mathrm{d}\sigma(\theta, \phi, z)}{\mathrm{d}\Omega}\right)_{\mathrm{Trig}}$$

be the differential cross section for an outgoing positron to emerge at a small angle θ and an azimuthal angle ϕ from a point z in the luminous region and, together with the recoil electron, satisfy all the trigger requirements for one of the four monitor channels. These requirements are (1) that the positron intersect the P counter, (2) that the recoil electron intersect the opposite C counter, and (3) that the energies deposited in both S counters, possibly including the energy of a radiated photon, exceed the S-counter threshold

energy. The radiative corrections $\delta(\theta, \phi, z)_{\text{Trig}}$ are then defined by the equation:

$$\left(\frac{d\sigma(\theta,\phi,z)}{d\Omega}\right)_{\text{Trig}} = \left(\frac{d\sigma_B(\theta,z)}{d\Omega}\right)[1+\delta(\theta,\phi,z)_{\text{Trig}}], \quad (7)$$

and in order to obtain the overall radiative correction it is necessary to integrate this expression over the angular acceptance of the P counter and over the intensity profile of the luminous region. This integration was carried out in terms of the variables u, v, z, where u and v are, respectively, the horizontal and vertical cartesian coordinates of the point at which the positron intersects the P counter (relative to the center of the P counter) and z is the longitudinal point of origin of the event (relative to the center of the luminous region). The radiative corrections $\delta(u, v, z)$ were computed for a matrix of 105 positron trajectories in the range $-0.25'' < u < 0.25''$, $0'' < v < 1.0''$ and $-14.5'' < z < 14.5''$. Due to the symmetry of the monitor under reflection about the horizontal plane, the relation

$$\delta(u, v, z) = \delta(u, -v, z)$$

was used to reduce the numer of computed trajectories. A representation of the form:

$$\delta(u,v,z) = \sum_{l=0}^{4}\sum_{m=0}^{4}\sum_{n=0}^{6} C_{lmn} u^l v^m z^n, \quad (8)$$

was found, where C_{lmn} are coefficients determined by the fitting procedure, and this representation was used in a numerical integration over the angular acceptance of the P counter and the intensity profile of the luminous region, as indicated in eq. (9).

$$\sigma = \iiint \frac{d\sigma_B(u,v,z)}{d\Omega}[1+\delta(u,v,z)]\, W(z) \times \times \frac{d\Omega(u,v,z)}{du\, dv}\, du\, dv\, dz, \quad (9)$$

where $W(z)$ is a normalized weighting function describing the intensity profile of the luminous region.

The magnitude of the overall radiative correction is summarized in fig. 6, which shows the total cross section for the acceptance of Bhabha events by the monitor, with and without the radiative correction, as a function of the fwhm of the circulating bunches. This figure also indicates the sensitivity of the computed cross sections to the betatron parameter β_v, which governs the vertical envelope of the circulating bunches. Both of the indicated values of β_v were used at various times during the experiment. The sharp decrease exhibited by all the cross sections for large widths of the circulating bunches arises, because Bhabha events can then occur at values of z so large that it becomes increasingly difficult, for geometrical reasons alone, for collinear or nearly collinear positrons and electrons to intersect the P and C counters, respectively. Under these conditions the radiative correction is harder to calculate with precision. There are two reasons for this difficulty. First, the radiative corrections $\delta(u, v, z)$ become large and change rapidly with u and v, and it becomes increasingly difficult to find a satisfactory functional representation for the matrix of $\delta(u, v, z)$. Second, the radiative corrections themselves, if computed to order α^3, are expected to be unreliable if they become large. The monitor was designed to operate for fwhm bunch lengths in the range 7–14″, which was the operating range anticipated during the design of SPEAR-I, so that its response would be very insensitive to the variation of the fwhm throughout the operating range. In fact, the fwhm bunch lengths at SPEAR-I turned out to be larger than expected, namely 17–22″, which brought the operating range of the monitor, as shown in fig. 6, closer than intended to the rapidly decreasing portions of the cross-section curves. Even so, the total cross section for Bhabha detection by the monitor is only expected to change by 0.5% over the operating range and the difficulties mentioned above are substantially avoided.

In order to probe the reliability of the computed radiative corrections, despite the unexpectedly large

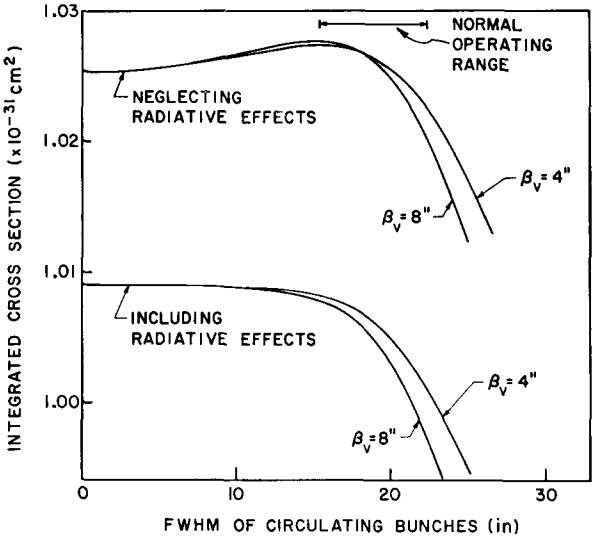

Fig. 6. The expected total cross section for Bhabha scattering integrated over the acceptance of one monitor channel as a function of the bunch length. The cross section is shown with and without the radiative correction and for two values of the vertical betatron parameter β_v. The range of bunch lengths encountered during normal operation is also indicated.

TABLE 2

The observed and calculated ratios of the rates in two monitor channels when the smaller counter C_4' is substituted for counter C_4. The ratios are shown for two values of the fwhm bunch length.

fwhm bunch length (inches)	Ratio $(P_2S_2)\cdot(C_4'S_4)/(P_2S_2)\cdot(C_4S_4)$	
	observed	calculated
14	0.965 ± 0.005	0.964
21	0.944 ± 0.003	0.947

bunch lengths, the monitor was operated for a short time with an additional counter C_4' placed close to the counter C_4. The dimensions of the smaller counter C_4' are given in table 1, and they are such that the potential difficulties referred to above in calculating the appropriate radiative corrections are substantially enhanced. The rates $(P_2\cdot S_2)\cdot(C_4'\cdot S_4)$ and $(P_2\cdot S_2)\cdot(C_4\cdot S_4)$ were measured simultaneously for two different values of bunch length, and their ratios compared with that expected from calculation. The results are shown in table 2. The agreement between measurement and calculation is good, and provides evidence that the radiative correction can be calculated reliably.

The computational accuracy of the overall radiative correction is expected to be better than 0.5%. Each of the third-order differential Bhabha cross sections provided by Berends et al.[4]), has a random computational error of 0.25%, while the average discrepancy observed between the chosen representation for $\delta(u, v, z)$ described by eq. (8) and a set of values of $\delta(u, v, z)$ computed for values of u, v, and z intermediate between those used to obtain the representation was 0.4%. The computed radiative correction was also shown to be independent, to within the computation error, of the S-counter threshold energy in the range 0.25–1.0 GeV, which makes the lack of definition in the threshold energy due to counter resolution unimportant. This is not surprising, because an event which is sufficiently collinear to be detected by the monitor is strongly restricted by kinematics to deposit a large fraction of the beam energy in each S counter, either from the electron or positron alone, or from an accompanying hard photon. The error due to the neglect of contributions to the Bhabha cross section of order higher than α^3 is not expected to be significant relative to the overall estimated accuracy of 0.5%. This is because radiative corrections involving soft photons can be well estimated to all orders of α by the replacement $\delta \to e^{\delta} - 1$, and approximately so for hard-photon processes. The relative error in δ computed to order α^3 should therefore be only of the order of δ itself.

6. Evaluation of the monitor response

The rates in the four monitor channels were individually recorded throughout the experiment and, although their sum is insensitive to displacements and rotations of the luminous region and to changes in its fwhm, the ratios of the rates in the individual channels can be used to reveal certain of these motions, should they occur. For example, the ratio

$$r_1 = (L_1 + L_4)/(L_2 + L_3),$$

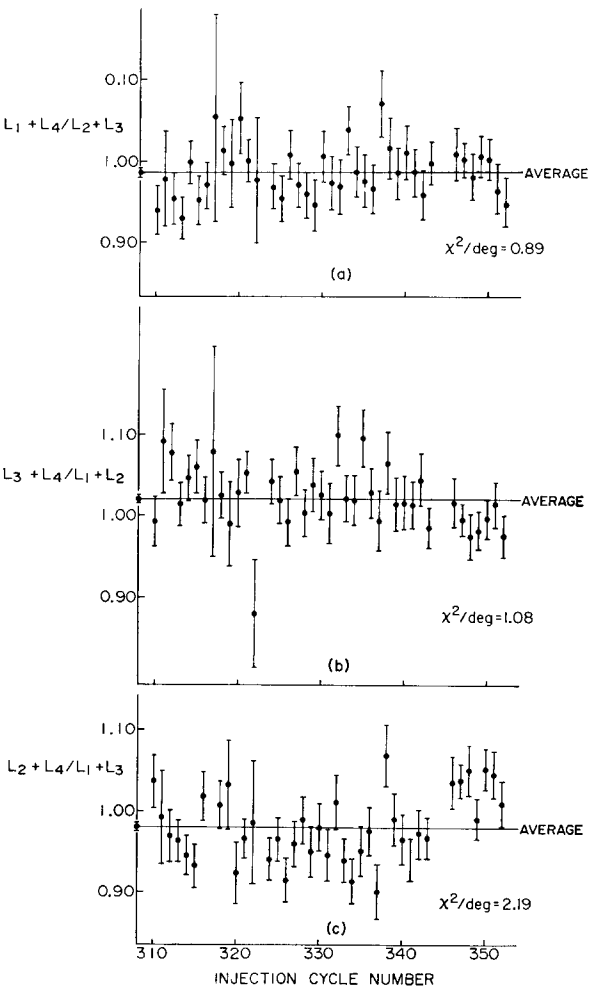

Fig. 7. The values of certain ratios of the rates observed in the four monitor channels for a typical sequence of 40 consecutive injection cycles. The ratio plotted in (a) is sensitive to displacements of the luminous region in the z direction, that in (b) to displacements in the x direction, and that in (c) to rotation around the y axis. For each ratio the value of chi-square per degree of freedom is calculated, assuming that the true value of the ratio does not change.

where L_1 is the rate $(P_1 \cdot S_1) \cdot (C_3 \cdot S_3)$ after the background correction, etc., is sensitive to displacements of the luminous region in the z direction. Fig. 7(a) shows the variation of the ratio r_1 for a typical sequence of 40 injection cycles. The expected value of r_1 is unity, because the luminous region cannot easily be displaced in the z direction. The observed average value of r_1 is 0.993 ± 0.005, and there is no statistical evidence, from a chi-square test, of movement of the luminous region in the z direction during this period. The ratio r_1 was used throughout the experiment as an indicator of normal operation of the monitor system.

Fig. 7(b) shows the ratio $r_2 = (L_3 + L_4)/(L_1 + L_2)$ for the same 40 injection cycles. This ratio, which is sensitive to displacements of the luminous region in the radial direction, has an average value of 1.020 ± 0.005, and reveals no significant radial motions of the luminous region during this period. The difference between the average value and unity is consistent with the uncertainty in the radial positions of the monitor counters relative to the equilibrium orbit of the beams.

Fig. 7(c) shows the ratio $r_3 = (L_2 + L_4)/(L_1 + L_3)$ for the same time interval. This ratio is sensitive to rotations of the luminous region around the y axis. The average value of r_3 is 0.981 ± 0.005, which is consistent with the uncertainty in the counter locations, but the data are not consistent with Gaussian fluctuations about this value. Instead, the data suggest the occurrence of random rotations of the luminous region with standard deviation of about 0.28 mrad during the observing interval. However, this is consistent with the expected degree of such rotations at SPEAR-I.

An analysis of the S-counter pulse heights, which were recorded for each monitor event, indicated the presence of a few percent of low-energy events (0.5–1.5 GeV) in each of the four monitor channels, which remained even after background subtraction. A typical S-counter pulse-height distribution is shown in fig. 8. The tail at low pulse heights was reduced almost to zero on $(P \cdot S) \cdot (P \cdot S)$ triggers, after background subtraction, and was not present in S-counter calibrations in a 2.6 GeV electron beam at SLAC. It appeared, therefore, that $(P \cdot S) \cdot (C \cdot S)$ events could be generated with low energies in either, or both, of the S counters in each channel. This signature can occur due to Bhabha events in which either, or both, of the Bhabha particles hit some part of the vacuum-chamber walls at a smaller than normal scattering angle. Such collisions generate secondaries which can then provide $(C \cdot S)$ or $(P \cdot S)$ coincidences with low S-counter pulse heights. This type of event is not removed by the background subtraction. Furthermore, because the small P counters are located at the center of the thin windows in the vacuum box, unlike the C counters which cover a much larger fraction of the area of the window, one would expect that such secondaries would be less likely to trigger the P counters than the C counters. It would then follow that those $(P \cdot S) \cdot (C \cdot S)$ triggers which are also $(P \cdot S) \cdot (P \cdot S)$ triggers ($\sim 25\%$) should give fewer low-energy pulses in the S counters. This is in accordance with observation. A correction for this effect can be made as follows. Inspection of the S-counter pulse-height distributions, for events in which the P counter of a particular monitor channel was involved, showed that energy cuts could safely be made at 1.2–1.4 GeV (compared to the hardware threshold of ~ 0.5 GeV). When such cuts were applied to both arms of the monitor channels, the correction to the luminosity became -3.0%, and the correction due to the spurious counts at higher energies in both counters was estimated to be about -0.3%. The uncertainty in the luminosity measurement due to this effect is conservatively estimated to be 1%.

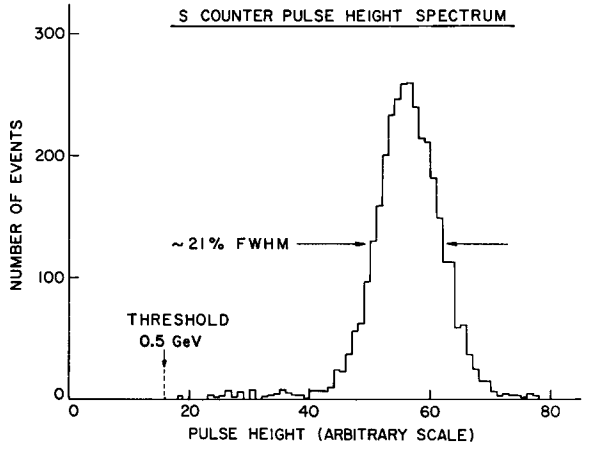

Fig. 8. A typical shower-counter pulse-height distribution for events accepted by the monitor, after subtraction of background events.

A second source of unwanted events not eliminated by the background subtraction occurs due to accidental coincidences between Bhabha events with the signature $(C \cdot S) \cdot (C \cdot S)$ and uncorrelated pulses in either of the two related P counters. $(C \cdot S) \cdot (C \cdot S)$ events typically occurred at the rate of about 3 per second, and pulses above threshold in each P counter at about 3×10^{-4} per beam crossing. Accidental coincidences of this type therefore occur in each monitor channel at the rate of about 10^{-3} per second, or approximately 0.5% of the rate of Bhabha events with the signature $(C \cdot S) \cdot (P \cdot S)$. The uncertainty in the luminosity incurred

TABLE 3

A list of all the known corrections and systematic errors larger than 0.1%. The total error is estimated by combining the individual errors in quadrature.

Source	Correction (%)	Uncertainty (%)
P Counter thickness	–	0.3
P Counter area	–	0.1
P Counter transverse separation	–	0.14
S Counter background	−3.3	1.0
P Counter accidentals	−0.5	0.5
Radiative correction	2.0	0.5
Total	−1.8	1.3

due to this correction is again conservatively estimated to be 0.5%.

A list of all known corrections and systematic errors greater than or equal to 0.1% is given in table 3. The overall systematic error on the response of the monitor is estimated to be less than $\pm 2.0\%$. This accuracy is entirely satisfactory for the purposes of the experiment at large angles, since the minimum statistical error achieved on the reactions observed at large angles was 3.0%. The largest experimental correction to the luminosity measurements is associated with Bhabha events which fall outside the normal acceptance of the monitor channels, but which themselves generate the background radiations necessary to cause monitor events. This source of error is not fundamental. If it can be suppressed, it then appears that the accuracy of the luminosity measurements that can be obtained through the application of the operating principles described in this paper to storage rings such as SPEAR-I approaches a limit set by the reliability with which the radiative correction can be calculated. This limitation appears to be within the design goal of $\pm 2\%$ at SPEAR-I.

7. Future applications

Prior to operating a precision luminosity monitor of the type outlined above at a different storage ring, such as SPEAR-II, consideration should be given to the effect of possible differences in the parameters of the new ring. Also the opportunity can be taken to incorporate changes in either the design or the operating procedure of the monitor that will assist in the interpretation of its response. In the former category, the principal difference between SPEAR-I and SPEAR-II, apart from the increase in the energy, is the expectation that the longitudinal fwhm of the luminous region will be reduced by a factor of 7 at SPEAR-II due to the use of a higher rf accelerating frequency. This will permit the P-counter acceptance to be increased for the same C-counter size, and so provide an increased counting rate. In the second category, the background related to low-energy pulses in the S counters, due to shower products from Bhabha particles outside the true acceptance aperture, can either be reduced by increasing the diameter of the thin windows in the vacuum box or by increasing the energy resolution of the S counters. The use of NaI(Tl) shower counters, for example, would provide an increase by one order of magnitude in the S-counter energy resolution. Measures can also be taken to reduce the luminosity error due to background pulses in the P counters in accidental coincidence with Bhabha events with the signature $(C\cdot S)\cdot(C\cdot S)$, which could become important if the P-counter background rates increase substantially. At least, the instantaneous rate of accidental events of this type should be monitored by continuously recording the P and $(C\cdot S)\cdot(C\cdot S)$ rates. Finally, no matter what modifications, if any, are made to the basic monitor system, it will be advisable for diagnostic purposes to record the pulse heights in all the monitor counters for each event and, in addition, to record at a suitable frequency the pulse heights in all counters in association with random beam crossings. In this way the signatures and correlations for all background sources can be inspected and all possible types of accidental rates can be computed correctly.

The authors gratefully acknowledge the support and assistance of their colleagues B. L. Beron, R. L. Ford, R. Kose, P. LeCoultre, T. W. Martin, L. Resvanis, R. F. Schilling and J. W. Simpson during the operation of the luminosity monitor at SPEAR-1. Acknowledgments are also due to Mr N. Dean of SLAC for his cooperation in the design of the vacuum box and for his supervision of its construction, to Dr R. Gastmans of the University of Leuven for assistance in adapting his computer codes to the calculation of our radiative corrections, and to Dr J. M. Paterson of SLAC for a critical reading of the manuscript. Finally, thanks are due also to Prof. Robert Hofstadter for his interest in this project.

References

1) The use of the single- and double-bremsstrahlung reactions in luminosity monitors is discussed by S. Tazzari, Frascati Report LNF-67/23 (1967).

2) G. E. Fischer, SPEAR Technical Note no. 154 (December 1972).

3) G. Barbiellini, B. Borgia, M. Conversi and R. Santonico, Atti Accad. Naz. Lincei **44** (1968) 233.

4) F. A. Berends, K. J. F. Gaemers and R. Gastmans, Nucl. Phys. **B68** (1974) 541.